Materials Science and Engineering B 151 (2008) 95–100

Contents lists available at ScienceDirect

Materials Science and Engineering B

journal homepage: www.elsevier.com/locate/mseb

Possible explanation for trapped field enhancement on REBaCuO bulk by modified multi-pulse technique with stepwise cooling (MMPSC)

H. Fujishiro [a,*], T. Hiyama [a], T. Naito [a], T. Tateiwa [a], Y. Yanagi [b]

[a] Faculty of Engineering, Iwate University, 4-3-5 Ueda, Morioka 020-8551, Japan
[b] Imra Material R&D Co. Ltd., 5-50 Hachiken-cho, Kariya 448-0021, Japan

ARTICLE INFO

Article history:
Received 11 October 2007
Received in revised form 4 March 2008
Accepted 4 March 2008

Keywords:
Pulse field magnetization
Bulk superconductor
Viscous force
Pinning force
MMPSC method
Temperature rise

ABSTRACT

The time evolutions of the local fields $B_L(t)$ have been measured on the surface of the superconducting bulk disk magnetized by a two-stage pulse-field magnetizing technique, called a modified multi-pulse technique combined with stepwise cooling (MMPSC), and the magnetic flux movement and the flux trapping have been investigated. The optimum concaved ("*M-shaped*") trapped field profile, which is a necessary condition at the first stage to enhance the final trapped field B_T, makes a larger magnetic gradient (dB/dx) at the bulk periphery in the ascending stage of the applied magnetic pulse at the second stage due to the large viscous force F_v. The magnetic fluxes, which stay at the bulk periphery, start to flow to the center of the bulk, after the applied pulse field reaches a maximum, at which the flux velocity v is nearly zero and then F_v decrease. As a result, a large number of the magnetic fluxes are trapped at the bulk center. The effect of the "M-shaped" profile at the first stage in MMPSC on the enhancement of B_T is discussed.

1. Introduction

Recently, a pulse field magnetization (PFM) for REBaCuO bulks (RE: rare earth element and Y) has been intensively investigated for practical applications, instead of a field-cooled magnetization (FCM), because PFM is an inexpensive and mobile experimental setup with no use of a superconducting magnet. The trapped field B_T^P by PFM is, however, lower than that by FCM at temperatures lower than 50 K due to the large temperature rise by the dynamical motion of the magnetic fluxes. At 77 K, several approaches have been performed and succeeded to enhance B_T^P by an iteratively magnetizing pulsed-field method with reducing amplitude (IMRA) [1], a multi-pulse technique with stepwise cooling (MPSC) [2] and so on. We have systematically studied the time and spatial dependences of the temperature $T(t,x)$, local field $B_L(t)$ and the trapped field B_T^P on the surface of cryocooled REBaCuO bulks 45 mm in diameter during PFM for various starting temperatures T_s and applied fields B_{ex} [3–5]. To enhance B_T^P, the reduction in temperature rise ΔT is an indispensable issue. The lowering of T_s is also effective because the critical current density J_c and resultant trapped field B_T^P increase with lowering T_s. However, in the PFM technique, the lowering of T_s as low as 10–20 K is not necessarily effective because of the large heat generation due to the enhancement of pinning loss and the decrease in the heat capacity of the bulk [6]. Taking the obtained experimental results into consideration, we proposed a new PFM technique named as a modified MPSC (MMPSC), which consisted of the two-stage procedures [7]. In this technique, a small number of magnetic fluxes should be trapped on the bulk periphery for the reduction in ΔT at a first stage at $T1$ ($<T_c$), and the optimum pulse field $B2$ should be applied at a second stage at $T2$ ($<T1$). The "M-shaped" trapped field profile, which means the lower trapped field at the bulk center than that at the bulk periphery, is also necessary at the first stage to enhance B_T^P. Using the MMPSC method, we have succeeded a highest field trapping of $B_T^P = 5.20$ T on the ϕ45 mm GdBaCuO bulk, on which 3.6 T had been trapped by a single pulse application at 40 K [8]. $B_T^P = 5.20$ T is a record-high value by PFM to date. The MMPSC method has been proved to be a universal and effective method to enhance B_T^P using other bulks such as the ϕ45 mm SmBaCuO disk with different pinning ability [9], the rectangular-shaped GdBaCuO bulk (33 mm × 33 mm × 15 mm) [10] and the large GdBaCuO disk 65 mm in diameter [11]. In the previous study, we measured the time evolutions of the local fields $B_L(t)$ at three points on the bulk surface [8] and the two-dimensional trapped field profile just above 0.5 mm on the bulk for various B_{ex} and T_s [12]. It has been found that the "M-shaped" profile should be experimentally optimized to enhance B_T^P. However, there has been no reasonable explanation for the question, why the "M-shaped" profile is necessary at the first stage in MMPSC.

In this paper, we measure the time evolutions of the local fields $B_L(t)$ at several points on the bulk surface for various conditions in

* Corresponding author. Tel.: +81 19 621 6363; fax: +81 19 621 6363.
E-mail address: fujishiro@iwate-u.ac.jp (H. Fujishiro).

0921-5107/$ – see front matter © 2008 Elsevier B.V. All rights reserved.
doi:10.1016/j.mseb.2008.03.010

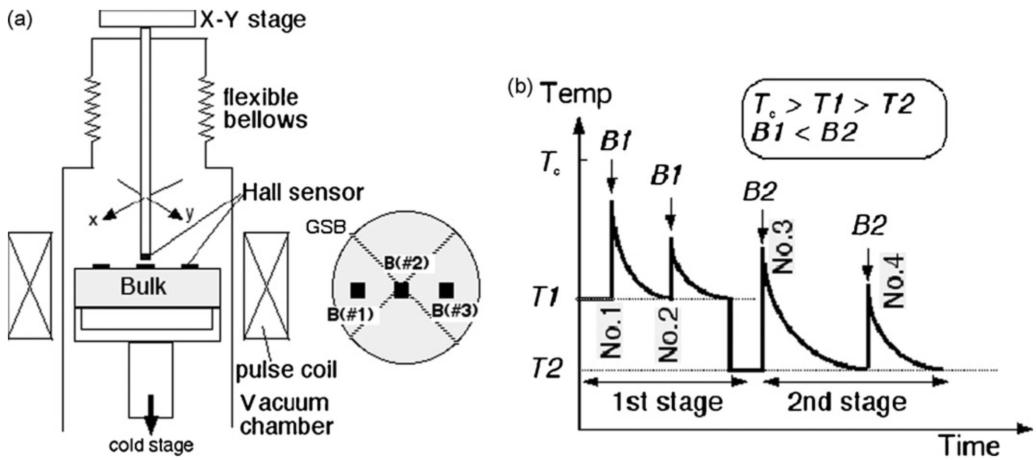

Fig. 1. (a) The experimental setup around the bulk and the pulse coil. Three Hall sensors are adhered at #1, #2 and #3 on the surface of the bulk. (b) The experimental sequence of the MMPSC method, where the estimated time dependence of the temperature is shown.

the MMPSC process, and analyze the magnetic flux movement and trapping. The meaning of the "M-shaped" profile at the first stage in MMPSC is discussed.

2. Experimental

The GdBaCuO bulk disk (Nippon Steel, Japan) used in this study was 45 mm in diameter and 18 mm in thickness, which was different from that attained B_T = 5.20 T [8]. Fig. 1(a) shows the experimental setup around the bulk and the magnetizing pulse coil. The bulk was mounted on soft iron yoke cylinder 40 mm in diameter and 20 mm in thickness and tightly anchored onto the cold stage of a Gifford–McMahon (GM) cycle helium refrigerator. The temperature of the bulk was controlled over the range from 30 K to 70 K. The magnetizing solenoid coil, which generated the pulse field up to B_{ex} = 6.3 T with a rise time of 12 ms, was placed outside the vacuum chamber, in which the central axis of the resulting field coincides with that of the bulk. The trapped field characteristics of the bulk by the single pulse application have been reported elsewhere [12]. Fig. 1(b) shows the experimental sequence of the MMPSC technique. Four magnetic pulses were applied at different initial temperatures *T*1 and *T*2 on the bulk surface. At the first stage, a pulse field *B*1 was applied twice at *T*1 (=70 K or 30 K) in order to realize various shapes of the trapped field profile on the bulk. Hereafter, we refer to these two pulses as Nos. 1 and 2. At the second stage, the bulk was cooled down to *T*2 (=30 K) and a higher pulse field *B*2 (=6.3 T) was applied twice (Nos. 3 and 4), after recovering to *T*2. Three Hall sensors (F.W. Bell, model BHT 921) were adhered in a line at the positions #2 (bulk center), #1 and #3 (12.5 mm distant from the bulk center) on the bulk surface as shown in Fig. 1(a). For each pulse of the MMPSC method, the time evolutions of the local fields [$B_L(\#1)(t)$, $B_L(\#2)(t)$ and $B_L(\#3)(t)$] were monitored by using a digital oscilloscope. The trapped field profile B_T(2 mm) was measured 2.0 mm above the bulk surface by scanning an axial-type Hall sensor (F.W. Bell, BHA 921) inside the vacuum chamber using a scanning device, which has an *x*–*y* stage controller with a flexible bellows. The trapped field profiles B_T(0.5 mm) were also measured 0.5 mm above the bulk surface under the same MMPSC conditions, after removing the adhered Hall sensors.

3. Results and discussion

3.1. Trapped field profiles at the first stage for various conditions

In the MMPSC method, a desired trapped field profile at the first stage can be controlled by choosing the conditions of *T*1 and *B*1, and the subsequent trapped field profile of the second stage is realized by *T*2 and *B*2. Table 1 summarizes four cases (Case A–Case D) and their conditions (*T*1, *B*1, *T*2 and *B*2) investigated in this study. Four trapped field profiles with different shape were realized at the first stage and, at the second stage, the magnetic flux movement and the trapping were measured after the pulse field application of *B*2 = 6.3 T at *T*2 = 30 K. In the Case D, the pulse fields were not applied at the first stage and the pulse field of *B*2 = 5.7 T was applied twice to the virgin state bulk at *T*2 = 30 K.

Fig. 2(a) shows the vertical sections of the B_T(0.5 mm) profile along different directions and the trapped fields [$B_T(\#1)$, $B_T(\#2)$ and $B_T(\#3)$] after applying pulse field of *B*1 = 3.2 T at *T*1 = 70 K (No. 1 pulse of the Case A). The two-dimensional B_T(0.5 mm) profile is also shown in the inset. The vertical sections are nearly symmetric, which suggest that the trapped field profile can be estimated using three Hall sensors at #1, #2 and #3. Fig. 2(b) shows the trapped field profiles from Case A to Case D at the end of the first stage. The measured B_T values at the positions from #1 to #3 and the estimated ones (B_T = 0) at the bulk edge (*X* = 22.5 mm) were used. In the Cases B and C, a "large M" and a "trapezoid" B_T profiles were realized, respectively. In the Case A, the M-shaped profile was somewhat smaller than that in the Case B, in which the maximum $B_T(\#2)$ as high as 4.0 T was finally obtained. We abbreviate the B_T profile in the Case A as "optimum M".

Table 1
The conditions (*T*1, *B*1, *T*2 and *B*2) and the final trapped field $B_T(\#2)$ from Case A to Case D in the MMPSC method

	1st stage (*T*1 and *B*1) (No. 1 and No. 2)	2nd stage (*T*2 and *B*2) (No. 3 and No. 4)	$B_T(\#2)$ (No. 4)
Case A (optimum M)	70 K, 3.2 T (No. 1) 70 K, 3.2 T (No. 2)	30 K, 6.3 T	4.0 T
Case B (large M)	30 K, 6.2 T (No. 1) 30 K, 6.2 T (No. 2)	30 K, 6.3 T	1.5 T
Case C (trapezoid)	70 K, 3.9 T (No. 1) 30 K, 4.6 T (No. 2)	30 K, 6.3 T	1.2 T
Case D (without)	–	30 K, 5.7 T	1.2 T

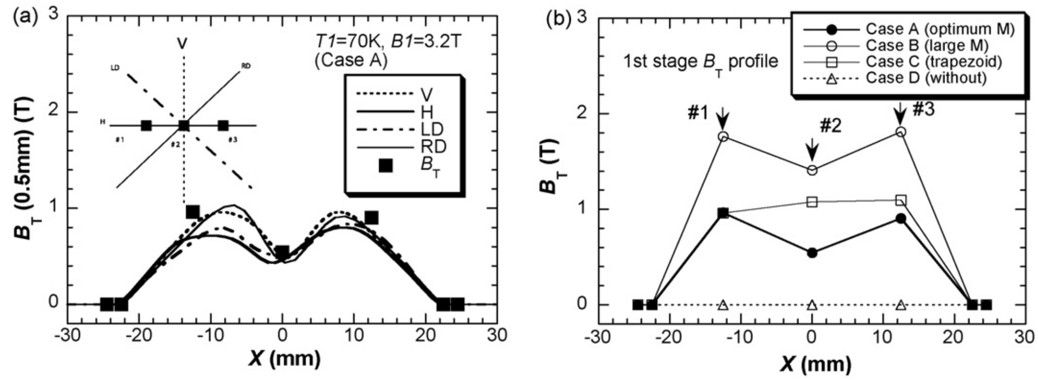

Fig. 2. (a) The example of vertical sections of the B_T(0.5 mm) profile along different directions and B_T at #1, #2 and #3 after applying pulse field of $B1$ = 3.2 T at $T1$ = 70 K. (b) The trapped field profile at the first stage in MMPSC method for the cases from Case A to Case D.

3.2. The flux movement and flux trapping at the second stage

The flux movement and the flux trap are investigated on the bulk with different trapped flux distribution from Case A to Case D, after applying the No. 3 pulse of $B2$ = 6.3 T (=5.7 T in the Case D) at $T2$ = 30 K. Fig. 3 shows the results for the Case A. In Fig. 3(a), the time evolutions of the applied field $\mu_0 H_a(t)$ and the local fields $B_L(t)$ at #1, #2 and #3 are shown. The applied field smoothly increased and took a maximum at t = 12 ms and then decreased. $B_L(\#1)(t)$ and $B_L(\#3)(t)$ started to rise at t = 6 ms with a time delay and took a maximum at t = 15 and 17 ms, respectively. $B_L(\#2)(t)$ started to rise at t = 13 ms with a long time delay, took a maximum at t = 17 ms and then decreased. The magnitude of $B_L(\#2)(t)$ is larger than that at #1 and #3 for t > 20 ms. Fig. 3(b) and (c) shows the time dependences of the transient magnetic distribution for the ascending ($t \leq$ 12 ms) and the descending ($t \geq$ 12 ms) stages of the No. 3 pulse field, respectively, both of which were reconstructed using $B_L(t)$ at #1, #2 and #3 shown in Fig. 3(a). $B_L(\#1)(t)$ and $B_L(\#3)(t)$ hardly change for $t \leq$ 6 ms and the magnetic flux distribution in the bulk showed a kink at #1 and #3. This result cannot be explained using a Bean's critical-state model under zero-field cooling, because the magnetic gradient dB_L/dx, which is proportional to a critical current density J_c, should be constant along the radius direction and the flux distribution should be expressed by a straight line. This result strongly suggests that the viscous force F_v for the flux movement is strong early in the ascending stage. For $t \geq$ 6 ms, $B_L(\#1)(t)$ and $B_L(\#3)(t)$ gradually increase and the flux distribution changes to a straight line. The $B_L(\#2)(t)$ value slightly increases during the ascending stage. For the descending stage as shown in Fig. 3(c), however, $B_L(\#2)(t)$ sharply increased at t = 15 ms, just after the applied field $\mu_0 H_a(t)$ took a maximum. $B_L(t)$ at #1 and #3 gradually decreased with increasing time and a cone-shaped trapped field distribution with $B_T^P = 4.0\,T$ was finally obtained.

Fig. 4 shows the similar results for the Case B, where a large M-shaped trapped-field profile was realized at the first stage. In Fig. 4(a), $B_L(\#1)(t)$ and $B_L(\#3)(t)$ started to rise at t = 6 ms and then took a maximum of 4.5 T at t = 13 ms. The maximum value was smaller, and the time, at which $B_L(t)$ took a maximum, was shorter than that for the Case A. In Fig. 4(b) and (c), $B_L(\#1)(t)$ and $B_L(\#3)(t)$ smoothly increased and then decreased. As a result, the large M-shaped profile was almost maintained. It should be noted that the magnetic gradient (dB_L/dx) at the end of the ascending stage (t = 12 ms) was smaller than that for the Case A.

Fig. 5 shows the similar results for the Case C, where a trapezoid-shaped trapped field profile was realized at the first stage. In Fig. 5(a), $B_L(\#1)(t)$ and $B_L(\#3)(t)$ keep the initial values up to t = 10 ms and then the magnetic fluxes abruptly intrude into the bulk like a flux jump. $B_L(\#2)(t)$ was not enhanced even at the descending stage, contrary to the Case A. In Fig. 5(b), F_v is strong for $t \leq$ 10 ms and magnetic fluxes cannot intrude into the bulk center. In the descending stage, $B_L(\#1)(t)$ and $B_L(\#3)(t)$ decreased with increasing time and the $B_L(\#2)(t)$ kept a initial value. Since the large temperature rise might take place at the bulk periphery due to the flux jump, the flux flow did not take place to the bulk center but took place to the bulk periphery. As a result, the $B_T(\#2)$ value was not enhanced only with a slight deformation of the trapped field profile.

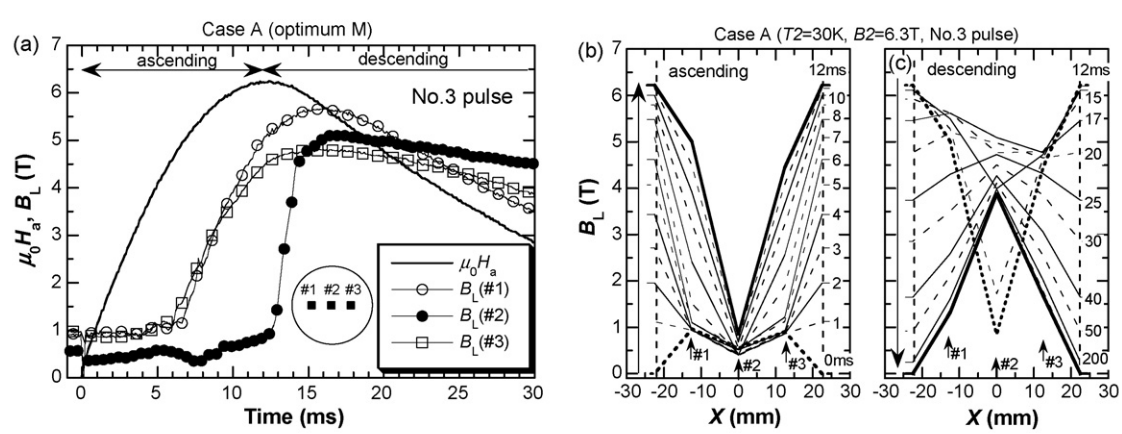

Fig. 3. (a) The time dependence of the applied field $\mu_0 H_a(t)$ and the local fields $B_L(t)$ at #1, #2 and #3 for the No. 3 pulse in the Case A (optimum M). The time dependence of the flux movement in the bulk for (b) the ascending ($t \leq$ 12 ms) and (c) the descending ($t \geq$ 12 ms) stages of the No. 3 pulse.

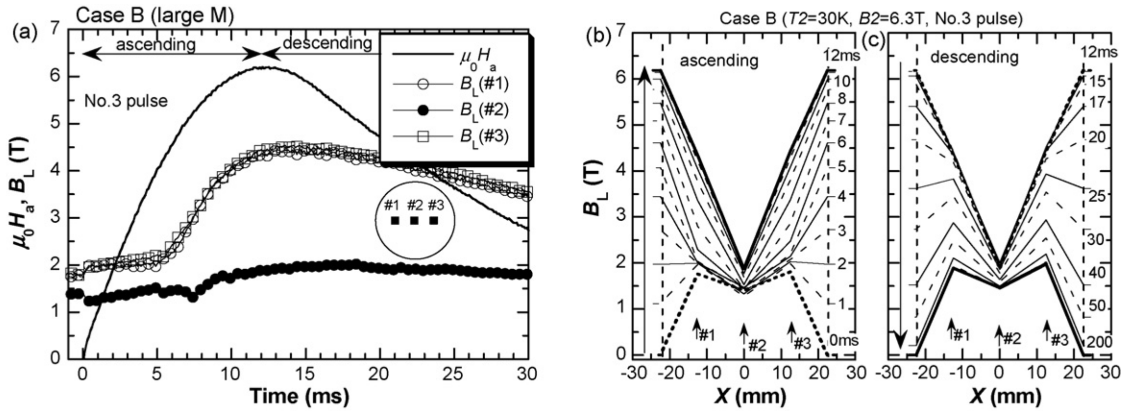

Fig. 4. (a) The time dependence of $\mu_0H_a(t)$ and $B_L(t)$ at #1, #2 and #3 for the No. 3 pulse in the Case B (large M). The time dependence of the flux movement in the bulk for (b) the ascending ($t \leq 12$ ms) and (c) the descending ($t \geq 12$ ms) stages of the No. 3 pulse.

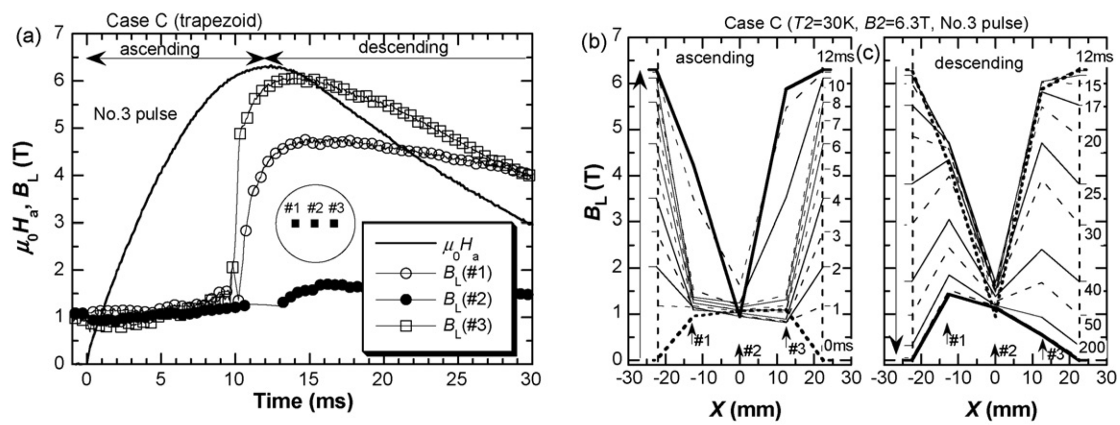

Fig. 5. (a) The time dependence of the $\mu_0H_a(t)$ and $B_L(t)$ at #1, #2 and #3 for the No. 3 pulse in the Case C (trapezoid). The time dependence of the flux movement in the bulk for (b) the ascending ($t \leq 12$ ms) and (c) the descending ($t \geq 12$ ms) stages of the No. 3 pulse.

The similar results for the Case D are indicated in Fig. 6, where a first magnetic pulse was applied to the virgin state bulk as a No. 3 pulse. In the previous paper, the temperature rise for the first pulse-field application is larger, compared with that in the case, where a small number of the magnetic fluxes are already trapped [5]. Then the maximum of $B_L(\#1)(t)$ and $B_L(\#3)(t)$ reaches 5 T and $B_L(\#2)(t)$ increases to 1.5 T due to the large temperature rise. In Fig. 6(b) and (c), the magnetic flux distribution is not a straight line along the radius direction at the end of the ascending stage, and finally shows the asymmetric M-shaped trapped field profile. The B_T^P value at the bulk center cannot be enhanced. These results from Figs. 3–6 suggest that the magnetic fluxes enter to the bulk center at the specified trapped field profile at the first stage.

3.3. Possible explanation of B_T enhancement in MMPSC

In the previous subsection, it was clarified that the optimum "M-shaped" profile such as "Case A" should be realized at the first

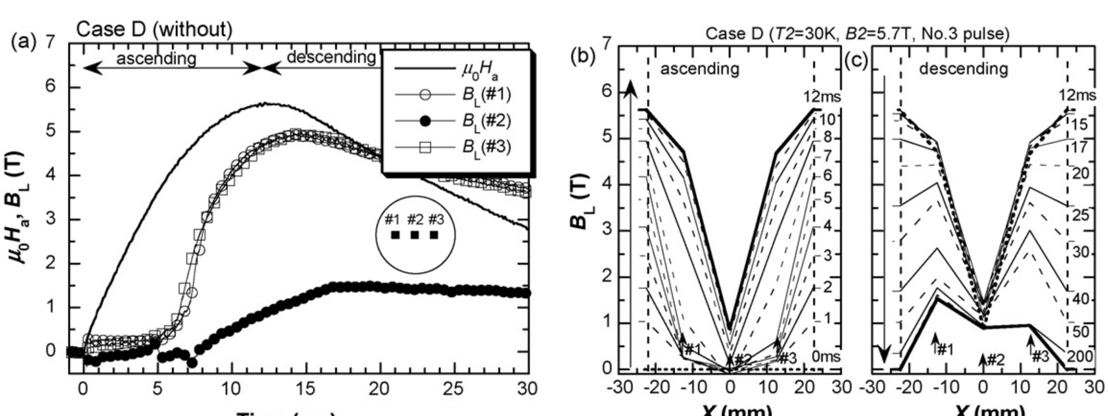

Fig. 6. (a) The time dependence of $\mu_0H_a(t)$ and $B_L(t)$ at #1, #2 and #3 in the virgin state bulk in the Case D (without). The time dependence of the transient magnetic distribution in the bulk for (b) the ascending and (c) the descending ($t \geq 12$ ms) stages of the No. 3 pulse.

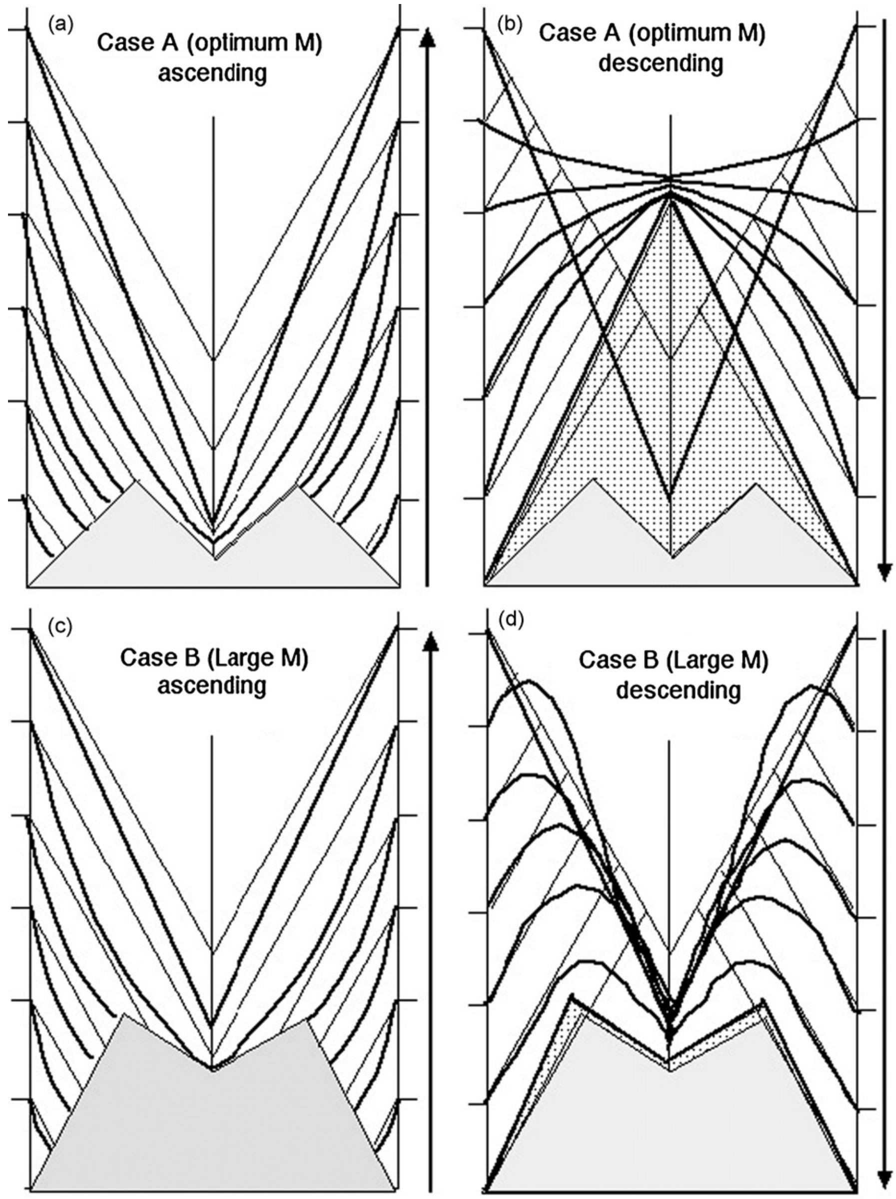

Fig. 7. The conceptual time dependence of the transient magnetic field distribution for the optimum M-shaped profile (Case A) ((a) and (b)), and for the large M-shaped profile (Case B) ((c) and (d)) for the ascending and the descending stages of the No. 3 pulse field.

stage in MMPSC to enhance B_T^P. We qualitatively discuss about the magnetic flux movement and trapping after the No. 3 pulse application, compared with the estimated results by a Bean's critical-state model.

The flux motion in the bulk is determined by the force balance in the critical-state model:

$$F_L = -(F_P + F_v) = J_c B + \eta \frac{B}{\phi_0} V, \quad (1)$$

where F_L is the Lorentz force, F_P the pinning force, J_c the critical current density, B the applied pulse field, η the viscosity coefficient, ϕ_0 a fluxoid quantum and v is the flux velocity. F_v is proportional to v, but F_P is independent of v.

Fig. 7(a) and (b) shows the conceptual time dependence of the transient magnetic field distribution for the optimum M-shaped profile (Case A) for the ascending and the descending stages of the No. 3 pulse field, respectively, both of which were estimated by use of the results in Fig. 3(b) and (c). In these figures, thin and thick lines show the distribution for the ZFC method (Bean's critical-state model) and for the No. 3 pulse application in the MMPSC method, respectively. In the MMPSC method, a large magnetic gradient (dB/dx) exists in the bulk periphery at the ascending stage, which is fairly larger than that estimated by a Bean's critical-state model due to the large viscous force F_v. When the applied pulse field reaches a maximum at $t = 12$ ms, a large number of magnetic fluxes, which stay at the bulk periphery, start to flow to the center of the bulk and then the trapped field profile changes from the "*M-shaped*" profile to the "*cone-shaped*" one at the descending stage. At this moment, the flux velocity v is nearly zero and F_v decreases to zero as estimated from Eq. (1). The magnetic gradient $\partial B(x,t)/\partial x$ in the bulk can be derived as follows [13]:

$$\frac{\partial B(x,t)}{\partial x} = \mu_0 \pm J_c \frac{B(x,t)}{|B|} + \frac{\eta}{\phi_0 |B| x_{x_0}}{}^{x} \frac{\partial B(x',t)}{\partial t} x' \, dx'. \quad (2)$$

In the ZFC method, since the time dependence of the magnetic field $\partial B(x',t)/\partial t$ in the bulk is almost zero, $\partial B(x,t)/\partial x$ is given by $\mu_0 J_c$. However, in PFM, the magnitude of $\partial B(x,t)/\partial x$ is markedly affected by the presence of the second term in Eq. (2). For instance, $\partial B(x',t)/\partial t$ is positive in the ascending stage and the second term of Eq. (2) becomes positive. Hence, $\partial B(x,t)/\partial x$ is enhanced by an amount relative to $\mu_0 J_c$ in the ZFC method.

Fig. 7(c) and (d) shows the similar conceptual view for the large M-shaped profile (Case B) for the ascending and the descending stages of the No. 3 pulse field. In this case, a large magnetic gradient (dB/dx) exists at the bulk periphery at the end of the ascending stage (t = 12 ms), but the dB/dx value is smaller than that for the optimum M-shaped profile (Case A) due to the higher height at the bulk center of the large M-shaped profile. Then the magnetic fluxes, which stay at the bulk periphery, do not flow to the bulk center, but flow to out of the bulk at the descending stage, even though the flux velocity v is nearly zero and the viscous force F_v decreases.

Finally, we comment on the influence of the temperature rise on the final trapped field during PFM. In the previous study, it was clarified that the already trapped fluxes in the bulk should reduce the temperature rise due to the decrease of the pinning loss Q_p [5]. In this study, the temperature rise seems to be the largest for Case D ("without") and is the smallest for Case B ("large M"), after applying the No. 3 pulse. The temperature rise for the Case C ("trapezoid") is estimated to be also large because of the flux jump. In this sense, a larger number of the magnetic fluxes should be trapped and the B_T(#2) value should be enhanced in the Case B. However, the B_T^P value was not enhanced for the Case B and the optimum "M-shaped" profile such as Case A ("optimum M") exists in MMPSC. These results strongly suggest that a moderate temperature rise is necessary to enhance the B_T^P value in the MMPSC method. The penetration of the field into the bulk during PFM could have been caused by a combination of heating due to the magnitude of the induced screening currents which corresponds to the slope of the B_L vs. x curve, and a suppression of J_c by the local field. It is necessary to study the flux dynamics using a theoretical treatment.

4. Summary

The time evolutions of the local fields $B_L(t)$ have been measured on the surface of the superconducting bulk disk magnetized by a modified multi-pulse technique combined with stepwise cooling (MMPSC) under various trapped field profiles at the first stage, and the magnetic flux movement and the flux trapping have been investigated. The important experimental results and conclusions obtained in this study are summarized as follows:

(1) The trapped field B_T^P by the MMPSC method strongly depends on the trapped field profile at the first stage. The "M-shaped" profile, which means the higher trapped field at the bulk periphery than that at the bulk center, is a necessary condition to enhance B_T^P and should be optimized.

(2) The time dependences of the flux distribution were reconstructed for the ascending and the descending stages of the applied pulse field using $B_L(t)$. These graphs enable us to understand the flux motion and trapping in the bulk clearly.

(3) Under the optimum M-shaped profile at the first stage, the large viscous force F_v is created at the end of ascending stage of the No. 3 pulse, at which the temperature rise is relatively small. When the applied pulse field reaches a maximum, at which the viscous force F_v decreases due to v = 0, a large number of magnetic fluxes, staying at the bulk periphery, start to flow to the center of the bulk and then the trapped field profile changes from the "*M-shaped*" to the "*cone-shaped*" one at the descending stage.

(4) A moderate amount of temperature rise is necessary to enhance the B_T^P value at the second stage, which is decided the relations between the trapped field profile at the first stage, $T2$ and $B2$.

Acknowledgements

The authors thank Professor T. Oka of Niigata University for the valuable discussions. This work is supported in part by a Grant-in-Aid for Scientific Research from the Ministry of Education, Culture, Sports, Science and Technology, Japan (No. 19560003).

References

[1] U. Mizutani, T. Oka, Y. Itoh, Y. Yanagi, M. Yoshikawa, H. Ikuta, Appl. Supercond. 6 (1998) 235–246.
[2] M. Sander, U. Sutter, R. Koch, M. Klaser, Supercond. Sci. Technol. 13 (2000) 841–845.
[3] H. Fujishiro, T. Oka, K. Yokoyama, K. Noto, Supercond. Sci. Technol. 16 (2003) 809–814.
[4] H. Fujishiro, K. Yokoyama, T. Oka, K. Noto, Supercond. Sci. Technol. 17 (2004) 51–57.
[5] H. Fujishiro, K. Yokoyama, M. Kaneyama, M. Ikebe, T. Oka, K. Noto, Physica C 426–431 (2005) 594–601.
[6] K. Yokoyama, M. Kaneyama, H. Fujishiro, T. Oka, K. Noto, Physica C 426–431 (2005) 671–675.
[7] H. Fujishiro, M. Kaneyama, T. Tateiwa, T. Oka, Jpn. J. Appl. Phys. 44 (2005) L1221–L1224.
[8] H. Fujisiro, T. Tateiwa, A. Fujiwara, T. Oka, H. Hayashi, Physica C 445–448 (2006) 334–338.
[9] H. Fujishiro, T. Tateiwa, T. Hiyama, Jpn. J. Appl. Phys. 46 (2007) 4108–4112.
[10] T. Tateiwa, Y. Sazuka, H. Fujishiro, H. Hayashi, T. Nagafuchi, T. Oka, Physica C 463–465 (2007) 398–401.
[11] H. Fujishiro, T. Tateiwa, K. Kakehata, T. Hiyama, T. Naito, Y. Yanagi, submitted to Physica C (2008).
[12] H. Fujishiro, T. Hiyama, T. Tateiwa, Y. Yanagi, T. Oka, Physica C 463–465 (2007) 394–397.
[13] Y. Itoh, U. Mizutani, Jpn. J. Appl. Phys. 35 (1996) 2114–2125.